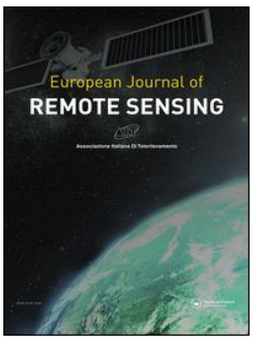

European Journal of Remote Sensing

ISSN: (Print) 2279-7254 (Online) Journal homepage: https://www.tandfonline.com/loi/tejr20

Modeling L- and X-band backscattering of wheat and tests over fields of Pampas

M. A. Acuña, P. Ferrazzoli & L. Guerriero

To cite this article: M. A. Acuña, P. Ferrazzoli & L. Guerriero (2019): Modeling L- and X-band backscattering of wheat and tests over fields of Pampas, European Journal of Remote Sensing, DOI: 10.1080/22797254.2019.1663711

To link to this article: https://doi.org/10.1080/22797254.2019.1663711

Published online: 05 Sep 2019.

EUROPEAN JOURNAL OF REMOTE SENSING
https://doi.org/10.1080/22797254.2019.1663711

Taylor & Francis
Taylor & Francis Group

Modeling L- and X-band backscattering of wheat and tests over fields of Pampas

M. A. Acuña[a,b], P. Ferrazzoli[a] and L. Guerriero[a]

[a]Dipartimento di Ingegneria Civile e Ingegneria Informatica (DICII), University of Rome Tor Vergata, Rome, Italy; [b]Comisión Nacional de Actividades Espaciales (CONAE), Buenos Aires, Argentina

ABSTRACT

A discrete scattering model and a detailed set of ground measurements are used to simulate the backscattering coefficients of wheat fields during the whole growth cycle. Simulations are carried out at L- and X-band, and at HH, VV, and HV polarizations. Wheat fields are located in Pampas (Argentina), and are characterized by low values of plant density. Simulations show that the backscattering coefficient is driven by variations of soil moisture at L-band, particularly for HH polarization, with low vegetation effects. Conversely, the attenuation of vegetation is dominant in producing variations of backscattering coefficients at X-band, particularly for VV polarization. Simulations are compared against experimental data collected over the same Pampas region, using airborne SARAT SAR at L-band and COSMO-SKYMED at X-band. Assuming a surface height standard deviation in a 0.4–0.7 cm range, the simulations generally agree with experimental data, with an RMSE lower than about 2 dB at L-band and X-band, except a limited number of cases. Discrepancies observed in specific conditions are discussed. Overall, the results indicate that a joint use of L- and X-band has a good potential to monitor both soil moisture and vegetation growth.

ARTICLE HISTORY
Received 26 January 2019
Revised 3 July 2019
Accepted 2 September 2019

KEYWORDS
Scattering models; SAR; crops

Introduction

The use of radar signatures of agricultural crops has been often quoted as a relevant application of microwave remote sensing. Recently, many experimental investigations using ground based and airborne instruments took place, providing a large amount of results. Further experiments were based on data collected by Synthetic Aperture Radar (SAR) mounted on satellites. In parallel, our understanding of the physical processes has been increasing, thanks to the development of backscattering models. The objective of all these efforts is the development of algorithms for retrieving soil moisture (SM) under crops, monitoring crop growth, and identifying vegetation status, with particular attention to the eventual conditions of water stress. An extensive review of experiments, applications, and modeling efforts, was recently provided by Steele-Dunne et al. (2017). The frequency range covering most of the experiments is between L-band (1.2 GHz) to X-band (10 GHz). The backscattering is contributed by three main sources: Direct backscattering from the soil, volume scattering from the vegetation canopy, interaction between soil and canopy. For developed crops, it is widely recognized that the relative weight of volume scattering increases with increasing frequency and angle, and is higher for cross-polarization. Moreover, crop stage is important, and many studies indicate that the amount of volume scattering is also dependent on crop type, since geometrical properties play an important role (Ferrazzoli, 2002). As a consequence of these considerations, L-band is preferred for soil moisture applications, and higher frequencies can help to improve the monitoring of biomass and vegetation properties. Some studies are aimed at producing simulations for global scale applications. An example is the work by Kim et al. (2014a), where "data-cubes" relating L-band backscattering coefficients to soil permittivity, soil root mean square (RMS) height and vegetation water content, were provided for broad vegetation classes.

Several studies are dedicated to wheat, due to its widespread presence in several climatic regions, and its alimentary importance. A fundamental requirement for applications is the decoupling between soil and vegetation effects. Kim et al. (2014b) used the Radar Vegetation Index (RVI), and assumed that this parameter was simply related to vegetation water content (VWC) and barely influenced by soil moisture. They achieved good correlations between RVI and VWC of various crops using measurements from a ground based scatterometer, particularly at L-band. However, Huang, Walker, Gao, Wu, and Monerris (2016) tested the same approach using airborne PLIS L-band data collected in Australia, obtaining less evident correlations. L-band SAR data collected by ALOS-PALSAR over Zwalm site and

CONTACT L. Guerriero leila.guerriero@uniroma2.it University of Rome Tor Vergata, DICII, Via del Politecnico 1, Rome 00133, Italy

E-SAR over DEMMIN site were analyzed by Lievens and Verhoest (2011). Measurements were collected during growth cycles of wheat fields, in the framework of the AgriSAR2006 campaign. This work was aimed at testing a SM retrieval algorithm based on the Integral Equation Model (IEM) for soil, with empirical vegetation correction based on Leaf Area Index (LAI) measurements. Temporal changes of soil moisture under crops were monitored by Balenzano, Mattia, Satalino, and Davidson (2011) using C- and L-band data collected by airborne SAR over the DEMMIN agricultural site (Northern Germany) during the European Space Agency 2006 AgriSAR campaign. A change detection algorithm, which can work over vegetated fields in case of low volume scattering, was proposed and tested over wheat and rape fields. Stamenkovic, Ferrazzoli, Guerriero, Tuia, and Thiran (2015) simulated L-band SAR signatures collected over wheat and corn fields using a discrete radiative transfer model. Then, SM was estimated using a nonlinear inversion technique based on the Support Vector Regression (SVR), trained by model simulations.

Although L-band is preferred for soil moisture monitoring, higher frequencies were also considered. Mattia et al. (2003) investigated the relationship of C-band backscatter measurements with wheat biomass and the underlying soil moisture content. Measurements were collected at HH and VV polarization and a wide range of incidence angles during the growing season using a ground-based scatterometer. Gherboudj, Magagi, Berg, and Toth (2011) proposed a soil moisture retrieval algorithm based on the model of Oh (2004) for soil and the Water Cloud model for vegetation correction. The method was tested using polarimetric parameters measured by C-band RADARSAT-2 over several fields, including wheat fields, in Canada. The sensitivity of SAR backscatter to crop and soil conditions was investigated by Moran et al. (2012) using 57 RADARSAT-2 quad-polarized SAR images acquired from April to September 2009 for large fields of wheat, barley, oat, corn, onion, and alfalfa in Barrax, Spain. The effects of changes of soil moisture and vegetation conditions at various polarizations were evaluated for different crops. Touré, Thomson, Edwards, Brown, and Brisco (1994) adapted the MIMICS model to simulate the signatures of wheat and canola at L- and C-band, VV and HH polarizations. Simulations were validated by comparisons with ground based scatterometer measurements. For wheat, the direct soil backscattering was dominant at L-band, but the contribution of canopy scattering was appreciable at C-band, particularly VV polarization.

A limited number of researches investigated the signatures of wheat at X-band, although this frequency shows a promising sensitivity to crop growth. Del Frate et al., (2004) reported decreasing trends of backscattering coefficients at S-, C-, and X-band as a function of wheat crop growth up to earing. The investigation was limited to HH and VV polarizations. The highest dynamic range of variation during the growth cycle of plants was observed at X-band. The experimental data set was used to test a radiative transfer model and a retrieval algorithm based on neural networks. Jia, Tong, Zhang, and Chen (2013) reported the measurements of the backscattering coefficients over wheat fields using an L-, S-, C-, and X-band scatterometer system during a whole period of wheat growth, in a site located in China. The fields were dense, with a maximum biomass exceeding 5 kg/m^2. In general the backscattering coefficient had a good correlation with biomass and leaf area index (LAI). In particular, the signatures at X-band confirmed the decreasing trend as a function of crop growth, and could detect newly transplanted thin wheat seedlings. Multitemporal, X-band signatures collected over Italian fields by COSMO-SKYMED SAR were used by Paloscia et al. (2014) to investigate the effects of crop growth for wheat and sunflower. At HH polarization, the trend of backscattering was increasing for sunflower, but it was decreasing for wheat also in this study. Simulations by a discrete radiative transfer model confirmed the observed properties at HH polarizations, and predicted the ones at VV polarizations, again characterized by a decreasing trend of backscattering coefficient during crop growth.

Experimental data and model simulations reported in the above referenced papers indicate that the attenuation of wheat canopies increases with frequency, incidence angle and crop growth, until earing. Moreover, the attenuation is higher at VV polarization than at HH polarization. At L-band wheat signatures are mostly driven by soil moisture, particularly at HH polarization. At the higher frequencies canopy attenuation produces a decreasing trend of backscattering coefficient versus crop growth, which is more evident at VV polarization. The ratios between cross-polarized and copolarized backscattering (HV/HH and HV/VV) generally increase during crop growth, but are also affected by geometrical factors. Moreover, for given configurations of frequency, polarization, and incidence angle, and for a given crop stage, the trends of wheat signatures are also affected by plant density. This parameter shows a wide range of variations related to environment and agricultural practices, ranging from minimum values of about 100 stems/m^2 to maximum values of several hundreds of stems/m^2. Some studies considered signatures collected over wheat fields with higher plant density, particularly at L- and C-band, but there is lack of data collected over fields with lower plant density, particularly at X-band.

In this paper, we simulate the backscattering coefficients during the cycle of wheat crops at L-

and X-band, HH, VV, and HV polarization. Simulations are obtained by adapting the model developed at Tor Vergata University (Bracaglia, Ferrazzoli, & Guerriero, 1995; Della Vecchia et al., 2006) to Argentinean wheat fields, using detailed ground data collected by intensive measurements in 2014 over a "reference" field representative of agricultural practices of the area. In Argentinean wheat fields the plant density shows low values, in a 100–200 plant/m^2 range. This modeling effort can have important outcomes, due to the different behavior of wheat at the two frequencies, already reported in previous papers. A joint use of L- and X-band can improve the simultaneous monitoring of soil moisture and vegetation properties. To this aim, simulations carried out by a discrete model are important to achieve understanding of multifrequency scattering processes and develop parametric investigations. The inclusion of X band in the analysis is particularly important, since investigations covering this frequency are sparse, although its sensitivity to crop growth can be useful.

Two validation data sets are used to assess the model performances. For L-band, we used airborne SAR data collected by SARAT instrument (Rava, Barber, Grings, & Karszenbaum, 2016; Skora, Sanz, & Fabbra, 2005) and ground measurements collected over six wheat fields in 2010 during the whole growth cycle. For X-band, we used ground measurements and signatures collected by COSMO-SKYMED over a large agricultural area in 2016. In both experiments, ground measurements covered soil moisture and general information about vegetation status, such as sowing date, plant density, and/or biomass. For both sites, the tests were carried out using the directly measured soil moisture, while detailed input vegetation variables required by the model were derived from the 2014 measurements over the reference field. Specifically, the latter were used to establish an empirical relationship between the vegetation variables and the day after sowing. This relationship was then applied to retrieve the vegetation variables in the test sites for a given day after sowing.

The sites are located in the region of Pampas, originally a temperate sub-humid grassland, which is the main cropland area of Argentina, where the main crops are soybeans, corn and wheat. Such a wide cropland is hard to be monitored with traditional in-situ techniques, while remote sensing can be appropriate. Moreover, this region will be continuously monitored after the launch of the Argentinian SAOCOM constellation of two satellites carrying aboard a polarimetric L-band SAR. The instrument is fully polarimetric, and operates at a resolution of 10–100 m, with an incidence angle in the range 17°-55°. The frequency will be 1.275 GHz. The revisit time will be 16 days for a single satellite and 8 days for the constellation of two satellites (http://www.conae.gov.ar/eng/satelites/saocom/cartecnicas.html).

A joint use of signatures made available by SAOCOM and COSMO-SKYMED is planned, in the framework of SIASGE agreement (Caltagirone et al., 2014). The next Section illustrates the experiments and the adopted model. Then, a parametric investigation and comparisons between model simulations and SAR measurements at both frequencies will be shown. Finally some concluding remarks will be drawn.

Materials and methods

The model and the reference data set

Backscattering coefficients at L- and X-band, and HH, HV and VV polarizations, were simulated using the discrete scattering model developed at Tor Vergata University. The general aspects of the model were described in detail by Bracaglia et al. (1995). Specific aspects related to the geometry of wheat were provided by Della Vecchia et al. (2006). The model represents the soil as a half-space with rough interface, and the wheat elements as discrete dielectric scatterers distributed in a lower layer with vertical cylindrical stems and leaves, and an upper layer with slightly inclined (10° from vertical) ears. Scattering contributions from all the components are computed using specific routines. For the soil, the permittivity was computed using the semiempirical model proposed by Dobson, Ulaby, Hallikainen, and El-Rayes (1985), and the integral equation model (IEM) (Fung, 1994) was used to evaluate the bistatic scattering coefficient, which is needed to compute the soil/vegetation interaction. Since IEM underestimates the crosspolarized backscattering (see, e.g. Choker et al., 2017), in this paper the HV component due to soil was empirically corrected by imposing the HV/VV backscattering coefficients ratios to be equal to the values reported by Oh (2004), for each frequency, angle, and SM value.

The $k\sigma$ product (k is the wavenumber, σ is the height std of surface) must be lower than 3.0 for IEM, and must be lower than 6.98 for the model of Oh (2004). For $\sigma < 1$ cm, both conditions are satisfied at L- and X-band.

The Rayleigh-Gans approximation (Eom & Fung, 1984) is used for discs, representing leaves, and the infinite length approximation (Karam & Fung, 1988) for cylinders, representing stems and ears. The single contributions are combined using the matrix doubling algorithm (Eom & Fung, 1984).

Dielectric and geometrical variables of vegetation required by the model as input were provided by detailed measurements carried out over a wheat field of the CETT (Centro Espacial Teófilo Tabanera) site, located near the

Argentinean city of Cordoba and owned by CONAE (Comisión Nacional de Actividades Espaciales). Measurements covered 12 dates of 2014.

The L-band experiment

The airborne SARAT instrument collected backscattering measurements in 2010 over agricultural fields at CETT site. SARAT is an L band (1.3 GHz) airborne SAR, flying at a nominal operational height between 4000 and 6000 meters above the terrain, with a noise equivalent backscattering coefficient of −40 dB . In 2010 SARAT flew over 20 agricultural fields at an incidence angle of 33°. The final images have a spatial resolution of 5.5 by 15.0 meters with 12 looks. The flights took place in seven dates, in which simultaneous measurements of SM, crop height and crop biomass were available. In this paper, we consider eight winter wheat fields, which can be grouped according to the different sowing dates: Day of year (DoY) 133, and DoY 151. Moreover, the site was subdivided into a Northern and a Southern area, each with four wheat fields. Northern fields are numbered 2, 4, 7, and 9. Southern fields are numbered 13, 16, 17, and 19. Information about azimuth directions of plant rows was also available. In the images used in this paper, the difference in azimuth between row directions and incident wave plane was about 32° for Southern fields and 50° for Northern fields. A map of the site, containing specific indications of wheat fields, is given in Figure 1. For each date and angle, several overpasses took place.

During the experimental campaign, ground measurements included fresh and dry biomass of vegetation and volumetric soil moisture. The latter was estimated using two measurements with TDR instruments and two gravimetric measurements for each field. Figure 2 reports average and standard deviations computed considering all SM measurements collected over wheat fields in each date as a function of the Day of Year. The rainfall is also reported. SARAT measurements of Day of Year 287 were collected a few hours after a rainfall event.

Measurements of biomass and vegetation water content (VWC) were only available for six fields. Increasing trends were observed until DoY 300, and the maximum VWC was moderate, in the range 0.5 to 0.8 kg/m^2. The plant density was 125 plants/m^2.

For soil roughness, we considered measurements of soil height standard deviation and correlation length carried out on the same CETT fields by Barber et al. (2016). These measurements were not simultaneous to SAR flights, but management practices of the fields were the same as in our experiment. For CETT fields the paper of Barber et al. (2016) reported a soil height standard deviation σ in a 0.4–1.0 cm range, a correlation length l in a 3.0–7.0 cm range, and a σ/l ratio around 0.15. We used this σ/l ratio and selected σ in order to obtain the best fit between SAR measurements and the model, in the range indicated by Barber et al. (2016).

The image pixels within each field were extracted using the maps and the associated backscattering coefficients. Six images were available on DoY 314,

Figure 1. Map of CETT site.

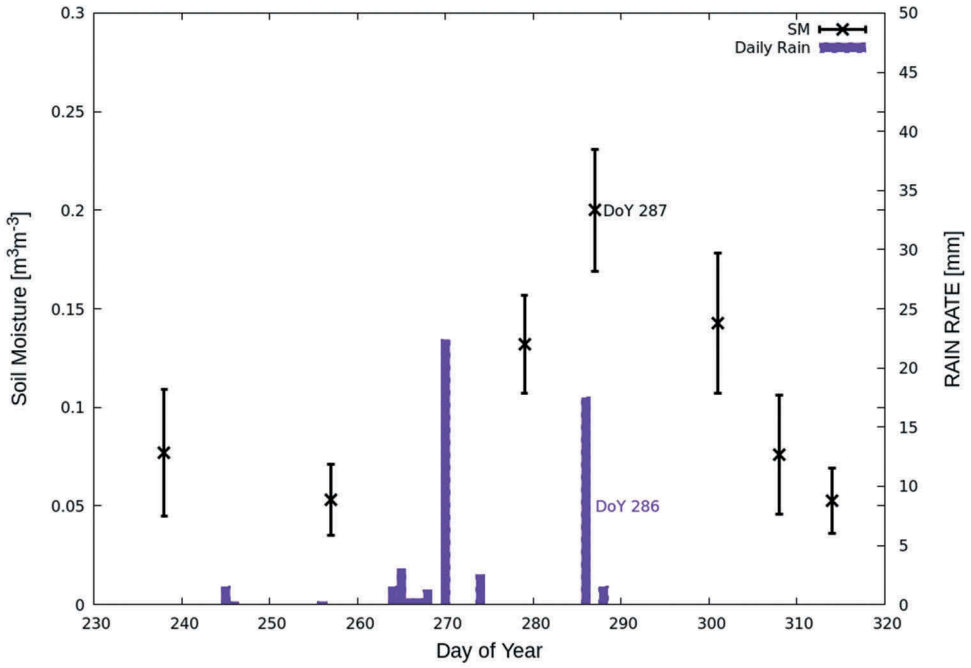

Figure 2. Temporal trend of soil moisture measurements over wheat fields during CETT 2010 campaign. Averages and standard deviations (error bars) are computed considering all measurements for each date. Vertical bars indicate rainfall.

9 on DoY's 287 and 301, 10 on Doy's 257, 279, and 308, and 20 on DoY 238.

Figures 3 and 4 report the backscattering coefficients measured over all images for the northern and southern fields, respectively.

The backscattering coefficients σ° of the northern plots were higher with respect to those of the southern fields. This finding can be related to the different azimuth angles between the directions of plant rows and the incident wave.

For testing L-band simulations, we used both soil moisture (SM) measurements and information about the sowing date collected during the flights in 2010. All the other crop parameters used by the model were found through empirical relations established on the basis of measurements collected in 2014 at the reference field and linking the vegetation variables to the number of days after sowing.

The X-band experiment

Available signatures at X-band were collected by COSMO-SKYMED SAR over wheat fields. The interaction of radar waves with wheat elements is weak at L-band, while it is important or even dominant at X-band. COSMO-SKYMED signatures have a short revisit time in Argentina, and nominally cover both co-polar and cross-polar signatures.

The site of Monte Buey, located in Pampas, was observed by COSMO-SKYMED in 2016. We analyzed and modeled signatures collected over five wheat fields. A map of the site is shown in Figure 5. The coordinates are 32°32′ S, 62° 65′ W for upper right corner, 32° 58′ S, 62° 01′ W for lower left corner. The fields analyzed in this work are labeled from "Wheat 1" to "Wheat 5". The size of the fields were around 1 km^2. The images analyzed here are from July 27th (DoY 206) to November 6th (DoY 310), covering most of the crop cycle, from early stage to dryness. However, most of the fields were destroyed by a heavy hailstorm, which took place on DoY 290.

During the observation time, the soil moisture was monitored at the site "La Valeria" located near the center of the area, using a Hydraprobe instrument with a sampling time of 1 hr. For soil roughness, we used the same method as in the case of CETT fields, since measurements of soil roughness by Barber et al. (2016) also covered the Monte Buey site, and the ranges of σ and l were similar to the ones of CETT.

COSMO-SKYMED operated at X-band (f = 9.6 GHz) in Ping-Pong configuration (Caltagirone et al., 2014). Signatures were collected at an angle of 40°, on the days and at the polarizations indicated below:

DoY 214, 222, 304: HH, VV;

DoY 246, 270: HH, HV;

DoY 206, 238, 251, 310: VV, HV.

The average backscattering coefficients in the five wheat fields were computed by averaging among the pixels belonging to each field, for each polarization. On average, the standard deviation with respect to averages was about 0.7 dB.

The trends of backscattering coefficients as a function of the time, in Julian dates, are reported in the upper part of Figure 6. The trend of measured soil moisture is reported in the lower part of the same figure. A general decreasing trend, more evident at

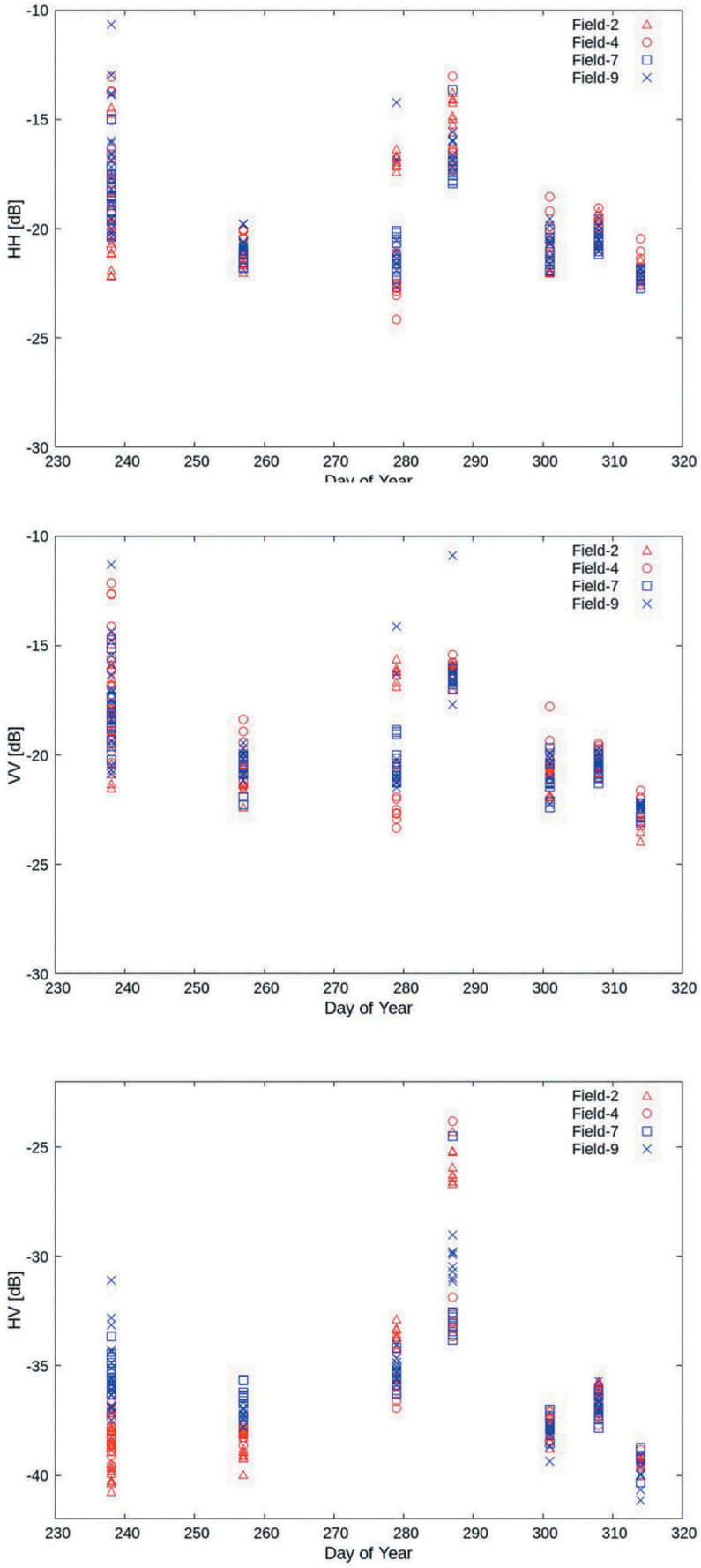

Figure 3. Temporal trend of backscattering coefficients measured at L-band at HH, VV and HV polarization over CETT 2010 northern fields. Fields were sowed on DoY 133 (blue), and DoY 151 (red).

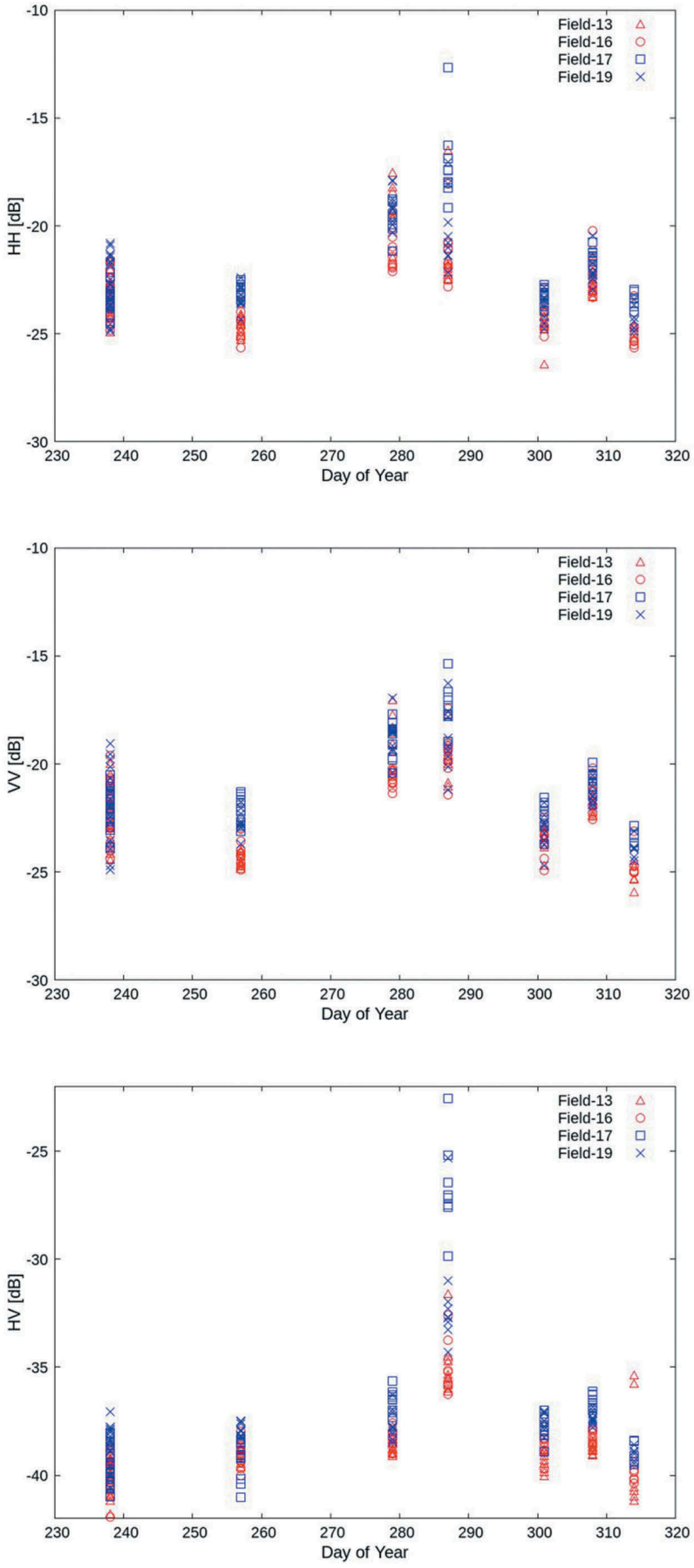

Figure 4. As in Figure 3 for southern fields.

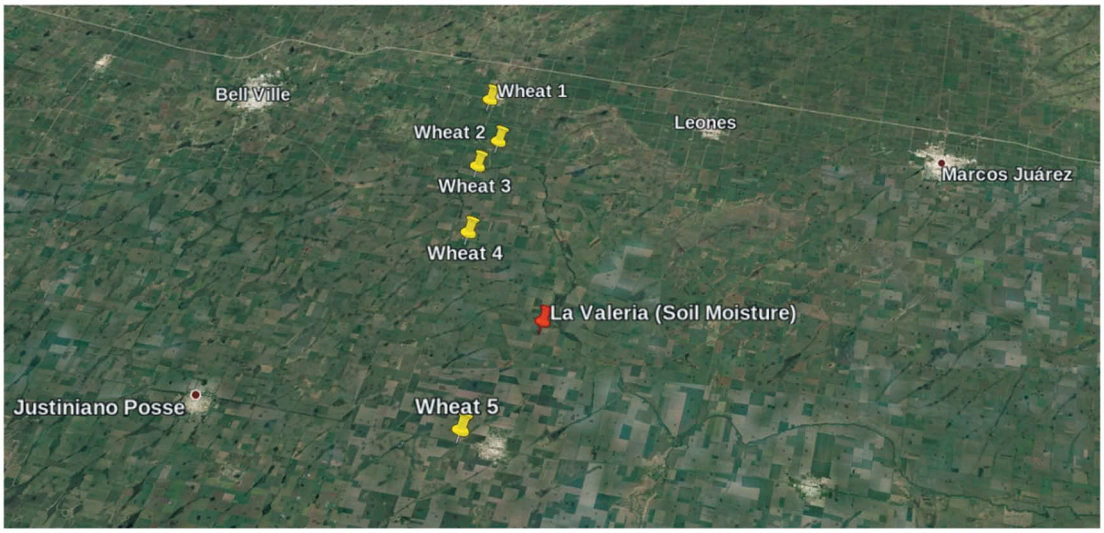

Figure 5. Map of Monte Buey site.

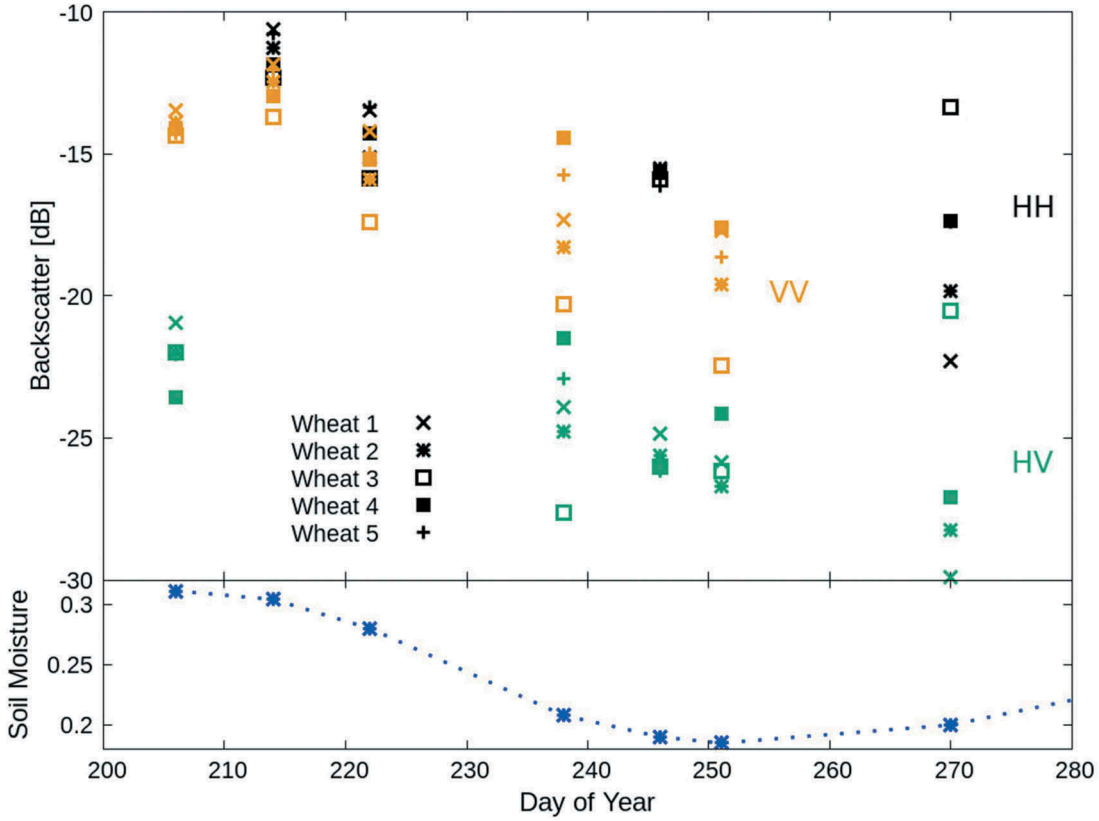

Figure 6. Top: temporal trends of backscattering coefficients of the five wheat fields measured by Cosmo_SkyMed in 2016. Bottom: Temporal trend of measured soil moisture.

VV polarization, is observed during the growing season. A model representation and interpretation of this property will be provided in the next Section. The soil moisture was also decreasing during the growth season, but the variation was moderate.

For testing X-band simulations we used soil moisture (SM) measurements taken at "La Valeria" station in 2016 during the flights. For the other crop parameters used by the model we used empirical relations based on the measurements collected in 2014 at the reference field for the same number of days after sowing. In this case, some fitting was applied since information about plant density was not available.

Summary of measurement campaigns

Information about measurement campaigns and their use in the procedure are summarized in Table 1.

Table 1. Measurement campaigns used in the procedure.

	2014	2010	2016
Site	CETT	CETT	Monte Buey
Relevant figures	7	1-4, 8-10	5-6, 11-13
SAR (Frequency band)	–	SARAT (L)	COSMO-SKYMED (X)
Angle	–	33°	40°
Polarizations	–	HH, VV, HV	HH, VV, HV
Number of fields	1	8	5
Soil moisture	–	Direct measurements	Direct measurements
Vegetation variables used as input to the model	Detailed measurements	Related to 2014 measurements for the same number of days after sowing	Related to 2014 measurements for the same number of days after sowing

Results

Parametric investigation

The obtained trends of the simulated backscattering coefficient for the reference field at 1.3 GHz and 9.6 GHz, as a function of the Day of Year (in 2014), are reported in Figure 7. The color codes indicate the different polarizations. There are two lines for each frequency and polarization, related to the conditions of dry soil (SM = 0.05 m^3/m^3) and wet soil (SM = 0.4 m^3/m^3). The surface height standard deviation σ is 0.5 cm, with a correlation length equal to σ/0.15. The corresponding trends of crop height and VWC are reported on top of the same figure. An angle of 32.5° was selected. At L-band, the dynamic range of simulated backscatter is mostly influenced by soil moisture, with a weak dependence on vegetation growth. Vegetation is almost transparent at HH polarization. At VV and HV polarizations a slight increase of backscattering is observed in full growth conditions, around Day of Year 290 due to volume scattering and, to a lesser extent, to double bounce produced by stems and ears. This effect disappears in the latest dates, due to drying. The simulated trends at X-band are completely different. At this frequency crop growth produces a strong attenuation, which lowers the backscattering coefficients and quenches the sensitivity to soil moisture at all three polarizations. The effect is particularly evident at VV polarization, since the vertical orientation of stems and ears produces a stronger interaction with radar waves. This result agrees with previous findings (Del Frate et al., 2004; Jia et al., 2013; Paloscia

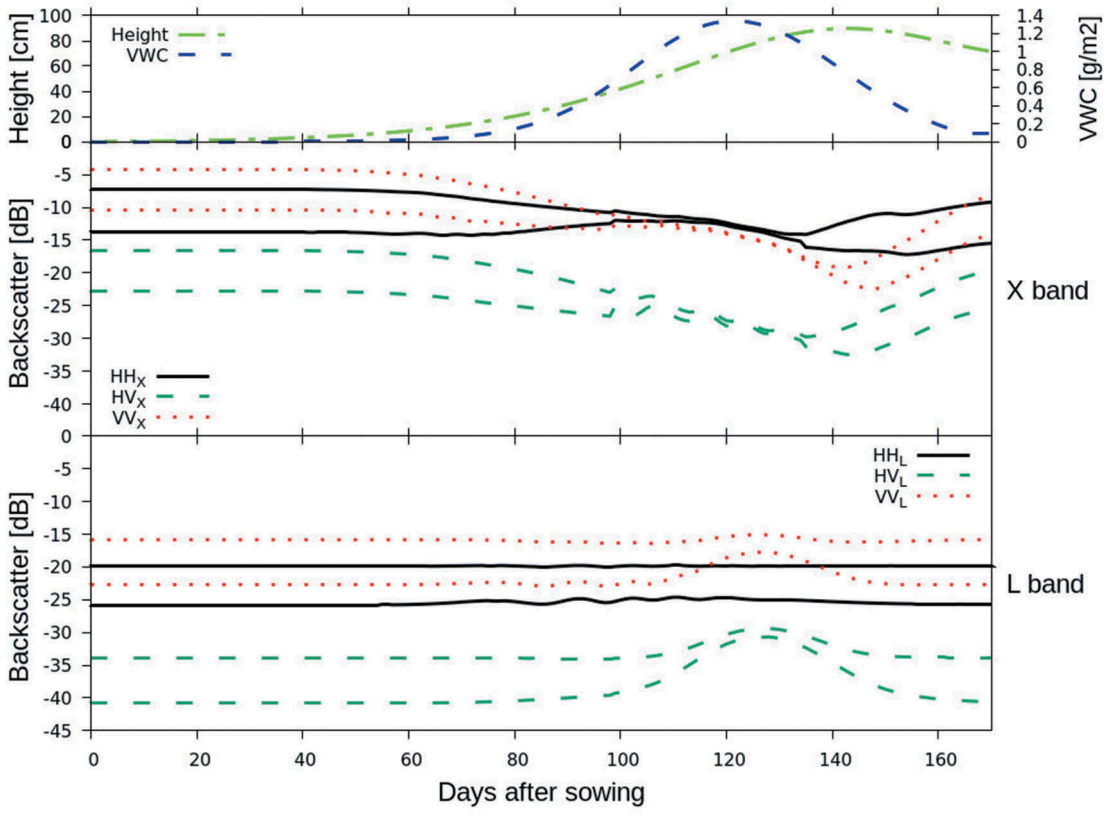

Figure 7. Top: Simulated trends of backscattering coefficient of the reference wheat field at CETT in 2014, as a function of the number of days after sowing. Top: Measured height (green line, cm) and VWC (blue line, kg/m^2). Middle: X-band. Bottom: L-band.

et al., 2014) obtained over fields with higher plant density. A decrease is also observed at HV polarization, in agreement with observations of Jia et al. (2013). Backscattering coefficients at all polarizations show a further decrease after earing, until about Day of Year 310, and increase again only in the last dates of advanced drying conditions.

Backscattering modelling tests at L-band

The multitemporal SARAT signatures collected in 2010 over the wheat fields have been compared against model simulations. Measurements of SM were used as a direct input. Due to the limited size of the test site, for each date we used a unique SM for all fields, which was obtained after averaging over all measurements of that date. The corresponding standard deviation was also used. Vegetation variables required by the model as input were fixed using the empirical function of the number of days after sowing, based on the 2014 measurements over the reference field.

Unfortunately, soil roughness measurements simultaneous to SARAT flights were not available. Then we evaluated the overall root mean square error between simulations and measurements as a function of soil height standard deviation σ (cm). The correlation length was again set equal to σ/0.15, according to the measurements reported by Barber et al. (2016). Results for VV polarization are reported in Figure 8. For all three southern fields the minimum RMSE is achieved for σ close to 0.5 cm, while for all three northern fields it is achieved for σ close to 0.65 cm. Both values are close to measurements from Barber et al. (2016). The minimum RMSE values are in the range 1.5–3.0 dB. We checked that similar trends and values are obtained at HH and HV polarization.

In order to have a picture of model performance in reproducing the backscatter temporal evolution, northern field 7 and southern field 16, which can be representative of behaviors of northern and southern fields, respectively, have been selected. Simulations have been done using the previously fitted values of roughness standard deviations σ. For each date, simulations were obtained using two soil moistures: the average measured one plus and minus the standard deviation. Results of a comparison between simulations and measurements are reported in Figures 9 and 10. For each date, the average and standard deviation of backscattering coefficients extracted from all available images collected over the considered field are reported. See Figures 3 and 4 for a resume of acquisitions.

For both fields, the simulated backscattering coefficients basically follow the trend of soil moisture reported in Figure 2. The maximum simulated value is achieved on Day of Year 287, for all polarizations. Measurements generally follow the same trend. However, the increase from Day of Year 279 to Day

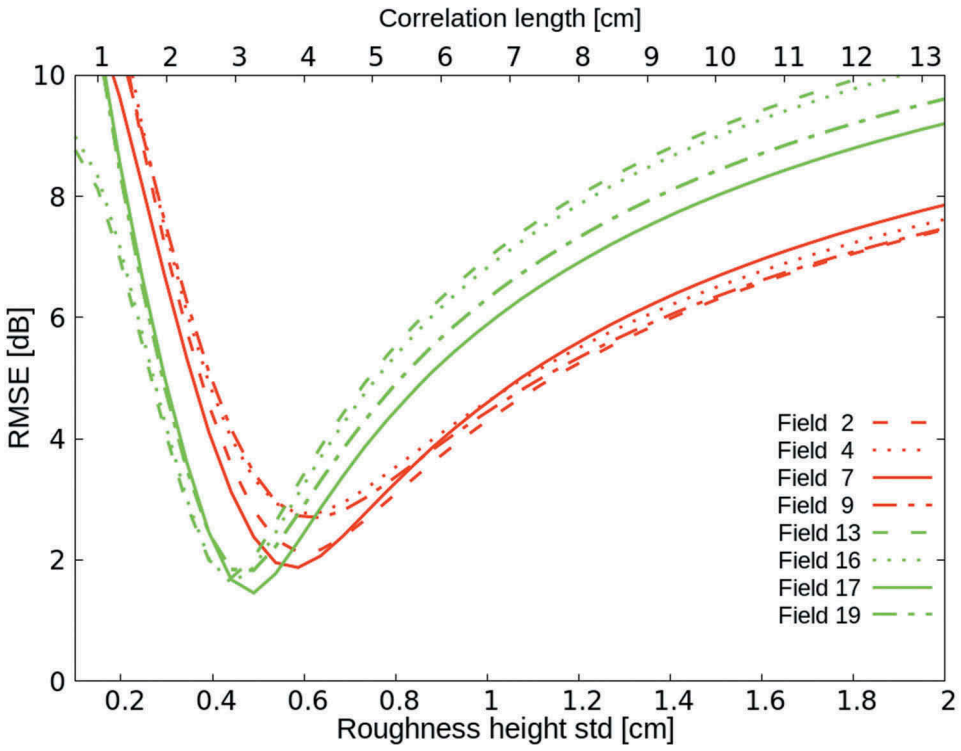

Figure 8. Overall RMS error between measurements and simulations of backscattering coefficient for each CETT 2010 field, as a function of roughness parameter σ used as input for each wheat field. Computations include all dates, at L-band and VV polarization.

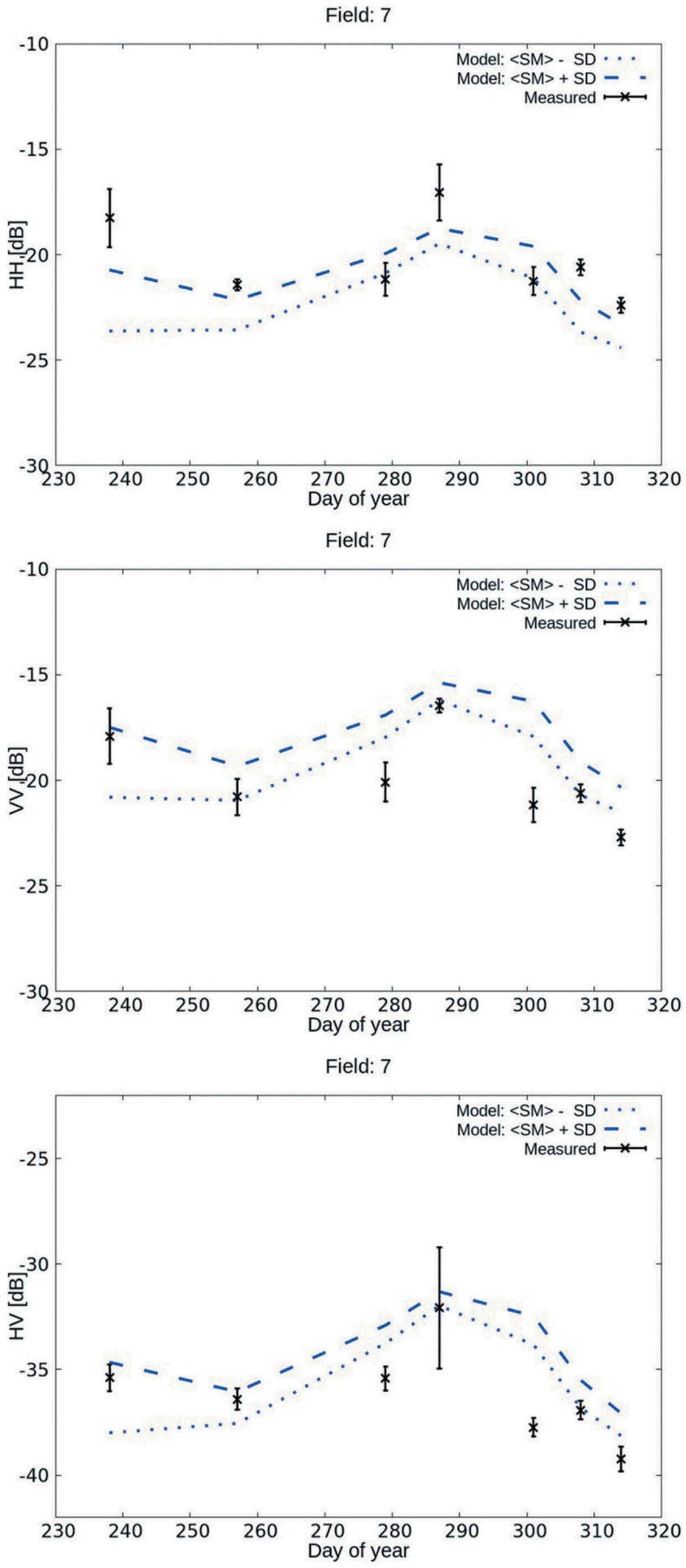

Figure 9. Temporal trend of CETT 2010 backscattering coefficients collected and simulated over wheat field number 7 (Northern field). Lines: Model simulations for a soil moisture equal to the average plus (dashed line) and minus (dotted line) standard deviation. Symbols: Average and std of SARAT measurements. Polarizations: HH (Top), VV (Middle), HV (Bottom).

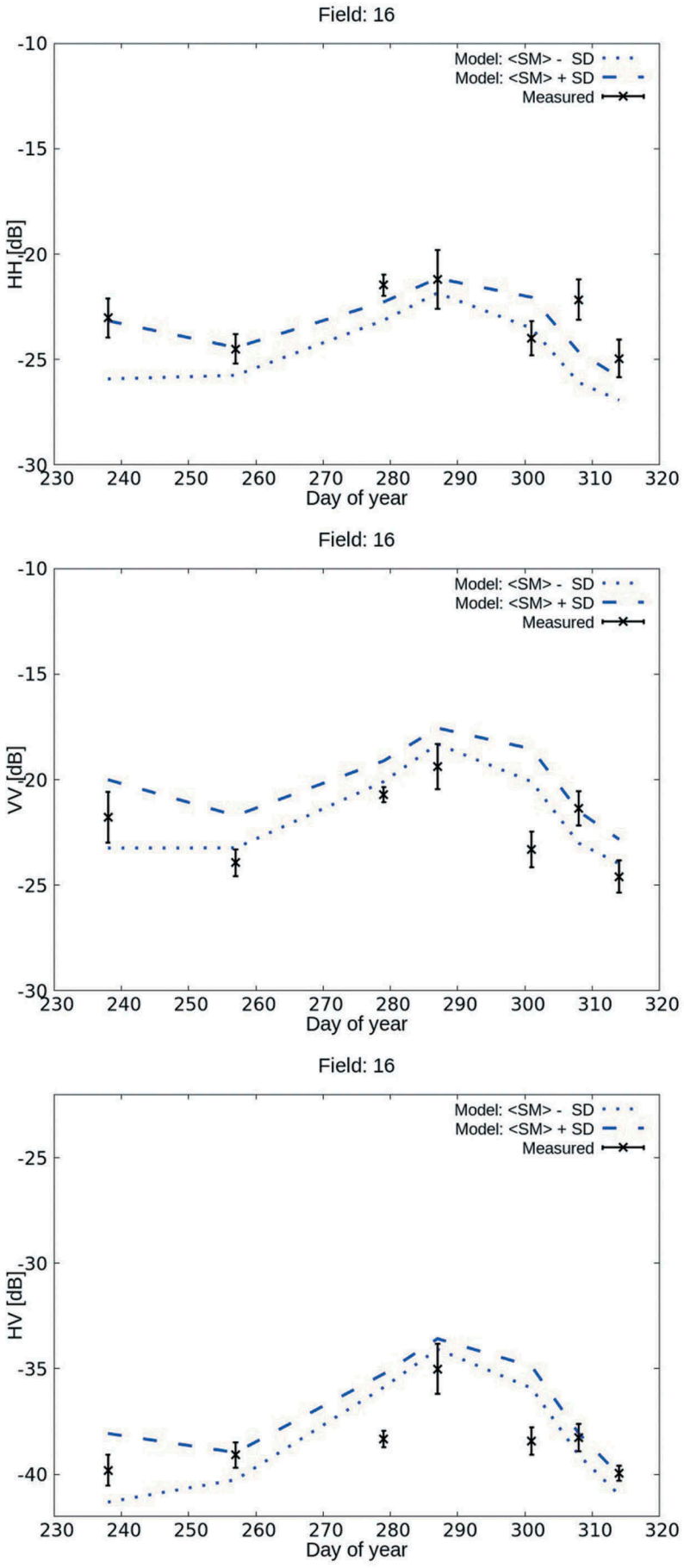

Figure 10. As in Figure 9 for field 16 (Southern field).

of Year 287 is either underestimated or overestimated. The flight of DoY 287 took place soon after a rainfall, and this can produce problems in the radar measurements and in the accuracy of SM representation. This is also confirmed by the higher standard deviations. Another discrepancy is observed on Day of Year 301 particularly in the southern field, which shows a decrease in backscattering, which is not followed by the model. Indeed, Figure 3 shows that there was a decrease in SM, but it was moderate. The field in the North shows a high range of backscattering coefficients at all polarizations in the first date. The acquisitions were carried out with different flight tracks and the model reproduces the lowest values among those observed. In all other cases the simulations are close to measurements.

Backscattering modelling tests at X-band

Model simulations were also compared against signatures collected at X-band by COSMO-SKYMED at Monte Buey site in 2016. The soil moisture measured at La Valeria site was used as input in the simulations for all five fields.

For some variables, we assumed possible variations within restricted ranges, based on the agricultural practices and environmental conditions of the area. The variables and corresponding ranges are indicated below.

Height standard deviation of soil roughness: 0.4–1.2 cm.

Sowing date (DoY): 100–120.

Plant moisture: As measured at the reference field in the same day after sowing ± 20%.

For the rest, detailed vegetation inputs were provided on the basis of measurements carried out at the reference field located in CETT for the same number of days after sowing.

First of all, we made the simulations at VV polarization, considering all the dates before the hailstorm for which this polarization was available, and computed the overall RMSE as a function of the assumed soil roughness parameter σ. The correlation length was equal to σ/0.15 in all cases. VV polarization was selected due to its higher dependence on crop growth, suggested by the trends reported in Figure 6. The computation was made for two cases of Julian sowing date: 100, and 110. The plant density was equal to 125 m^{-2}. Results are reported in Figure 11. Since the backscattering is dominated by volume during the growth cycle, the roughness parameter is not as critical as in case of L-band. For a Julian sowing date equal to 110, the values of RMSE are lower than 2.0 dB for all fields except field labeled as "Wheat 3". An opposite situation is observed for a Julian sowing date equal to 100. In this case all RMSE's suffer a clear increase, except field "Wheat 3", which shows a lowering RMSE below 2 dB. The number of days after sowing is a critical parameter, since controls the temporal trend of attenuation due to vegetation.

Following this result, we simulated the temporal trends of backscattering coefficients for a plant density equal to 125 plants/m^2 considering six cases: sowing dates equal to 100, 110, and 120, soil roughness σ equal to 0.4 cm and 1.0 cm. All polarizations were considered in their dates of availability. Results are reported in Figure 12. The model fits well the measurements at VV polarization. Most of the samples are located within an interval related to the assumed variation of the sowing date. During the growing phase, the effect of roughness variation is negligible, due to the high X-band attenuation. The decreasing trend is due to a balance between the scattering and attenuation properties of leaves and stems. At early stage, stems are very short, while leaves are developing and produce appreciable scattering. During the growth, the height of vertical stems increases, attenuating the scattering produced by the lower leaves. This effect is particularly important at VV polarization. At HH polarization the stem attenuation is weaker, the decreasing trend is less evident, and the effect of soil roughness is observed at earliest dates. In this case the model reproduces well the observations during the first three flights, but is unable to explain the lowering in the in the measurements backscattering observed for most of the fields in DoY 270, during the drying phase. At HV polarization there is a bias between simulations and measurements, although the trends are similar. HV backscattering is strongly influenced by some geometrical variables, such as inclination of leaves, stems and ears. However, the noise equivalent backscattering coefficient of COSMO SKYMED is −22 dB (Caltagirone et al., 2014), which makes the absolute calibration of HV signatures questionable in this range of measured values.

The comparison was made again by assuming fixed sowing dates and plant densities (DoY 110 and 125 plants/m^2, respectively) and considering possible variations of plant moisture. The height standard deviation of soil roughness is 0.4 cm. In particular, simulations were carried out assuming plant moistures with a variation of ± 20% with respect to the values measured at the CETT reference field for the same dates after sowing.

Results are reported in Figure 13. Variations of plant moisture produce some effects on simulated outputs.

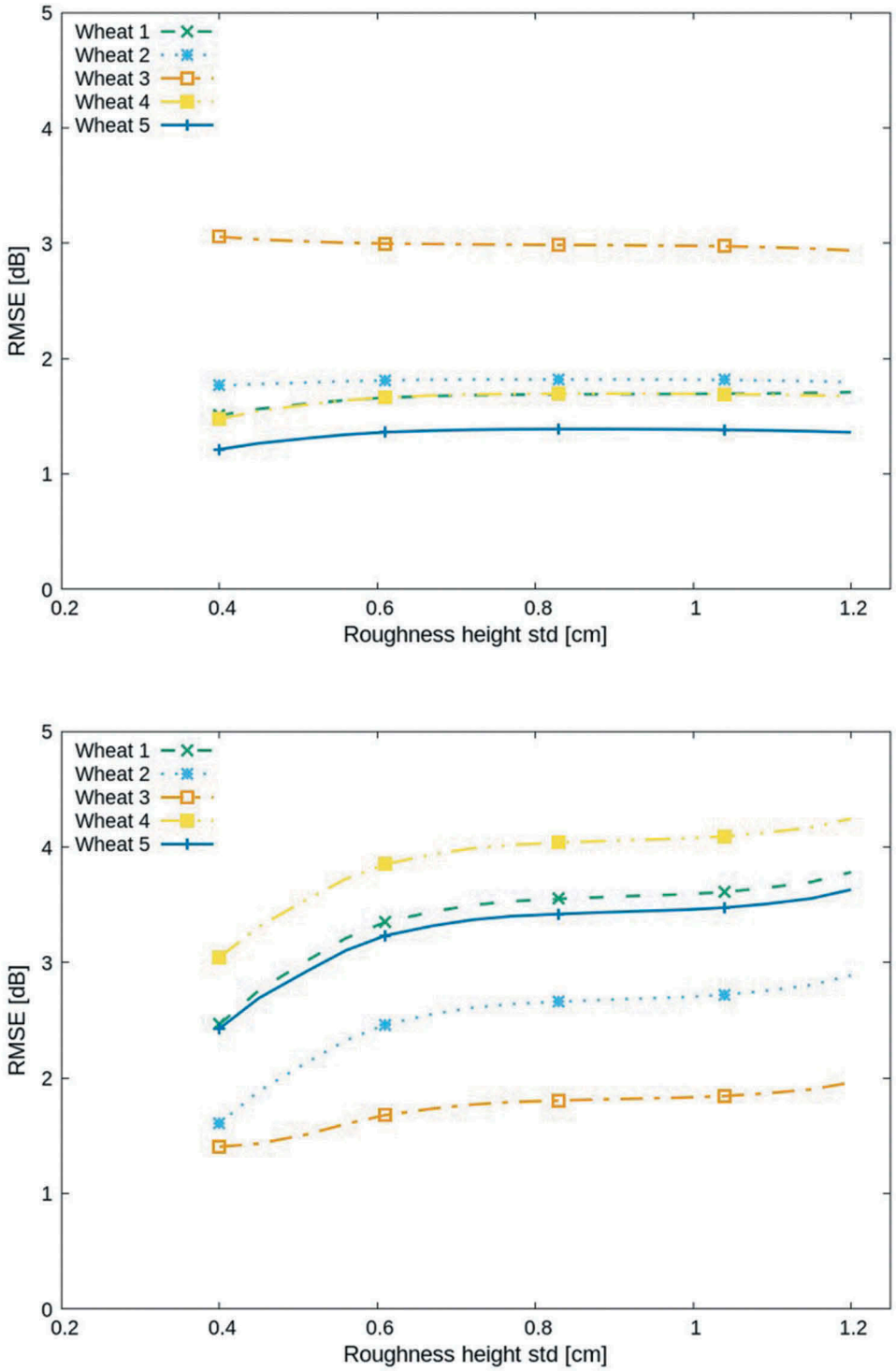

Figure 11. Overall RMS error between measurements and simulations of backscattering coefficient for five Monte Buey fields, as a function of roughness parameter σ used as input. Computations include all dates, at X-band and VV polarization. Plant density = 125 m^{-2}. Top: Julian sowing date equal to 110. Bottom: Julian sowing date equal to 100.

Overall, the most sensitive polarization is VV, the driving parameter is the sowing date. According to Figures 11–13, variations of plant moisture within realistic ranges produce effects comparable to variations of ± 5 days after sowing. The effects of soil roughness are low.

Conclusions

The discrete scattering model developed at Tor Vergata University has been used to simulate backscattering coefficients of wheat at L- and X-band, and at HH, VV, and HV polarizations, for the whole

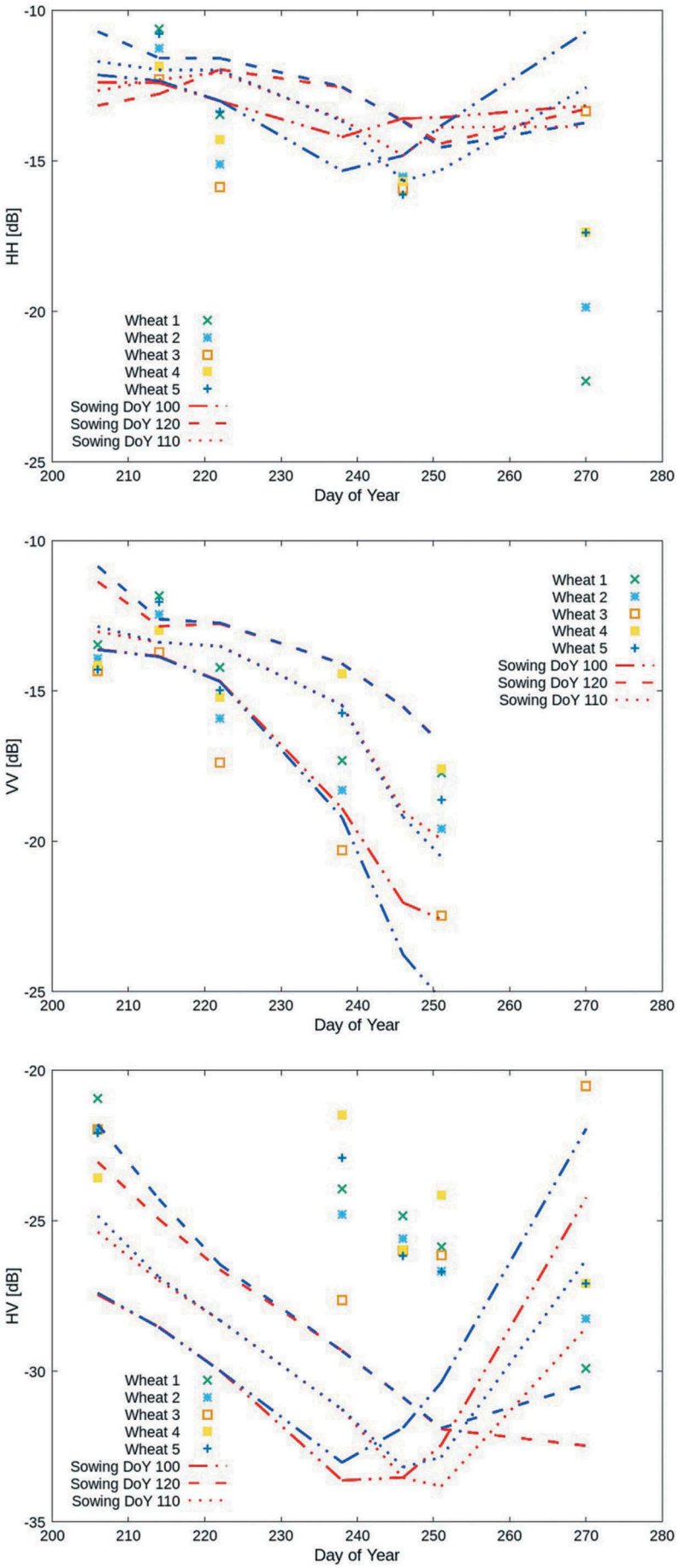

Figure 12. Multitemporal comparison between measured and simulated backscattering coefficients. Possible variations of soil roughness and sowing date are considered. Top: HH polarization; Middle: VV polarization; Bottom: HV polarization.

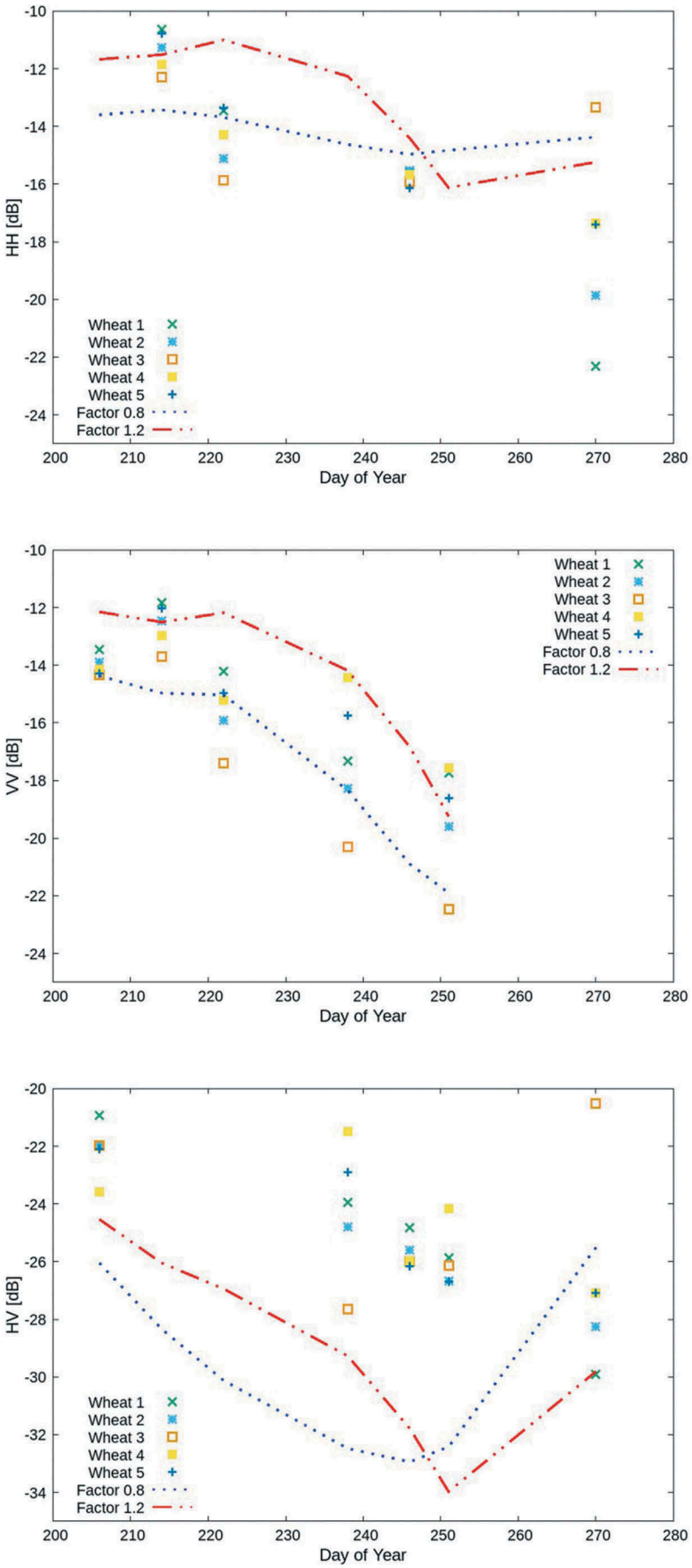

Figure 13. Multitemporal comparison between measured and simulated backscattering coefficients. Possible variations of plant moisture are considered. Plant moisture is 20% lower (Factor 0.8) or 20% higher (Factor 1.2) with respect to measurements at reference field. Soil roughness hstd: 0.4 cm. Top: HH polarization; Middle: VV polarization; Bottom: HV polarization.

growth cycle of wheat fields. Input data requested by the model have been provided by detailed measurements carried out over a wheat field of CETT site. According to Argentinean practices, the plant density (125 plants/m^2) was considerably lower with respect to wheat fields of different countries. As a consequence of this low density, vegetation effects predicted by the model are low at L-band, particularly in case of HH polarization. However, a strong attenuation is predicted at X band, particularly at VV polarization, during the growing phase and up to the first drying period. The model has been tested using airborne SAR signatures of SARAT instrument at L-band and COSMO-SKYMED signatures at X-band. Assuming a soil roughness height standard deviation in a 0.4–0.7 cm range, simulations generally agree with measurements. For most fields, the RMSE is lower than 2 dB at both L-band and X-band, VV polarization. At L-band, some critical issues are found for radar data collected soon after a rainfall. Moreover some effects of the azimuth angle, which can be critical in the exploitation of the radar measurements, have been observed. At X-band the worst discrepancies have been found at HV polarization, most probably related to the noise equivalent backscattering coefficient of COSMO-SKYMED.

Overall, the study demonstrates that a joint use of SAOCOM and COSMO-SKYMED can monitor the evolution of both soil moisture and vegetation properties of wheat fields in the Pampas region. For soil moisture, at L-band, HH polarization, angles lower than 40°, vegetation effects can be considered negligible, and the accuracy is determined by the soil model. For vegetation, the most useful configuration is X-band, VV polarization, angles lower than 40°. In this case the driving parameter is the sowing date. Variations of plant density and/or plant moisture within realistic ranges produce effects comparable to variations of ± 5 days after sowing.

Acknowledgments

Work supported by ESA (European Space Agency) under contract 4000117341/16/F/MOS in the framework of Alcantara initiative.

Disclosure statement

No potential conflict of interest was reported by the authors.

Funding

This work was supported by the European Space Agency [4000117341/16/F/MOS].

ORCID

L. Guerriero http://orcid.org/0000-0002-0812-1048

References

Balenzano, A., Mattia, F., Satalino, G., & Davidson, M.W.J. (2011). Dense temporal series of C- and L-band SAR data for soil moisture retrieval over agricultural crops. *IEEE Journal of Selected Topics in Applied Earth Observations and Remote Sensing*, *4*, 439–450. doi:10.1109/JSTARS.2010.2052916

Barber, M.E., Grings, F.M., Álvarez-Mozos, J., Piscitelli, M., Perna, P.A., & Karszenbaum, H. (2016). Effects of spatial sampling interval on roughness parameters and microwave backscatter over agricultural soil surfaces. *Remote Sensing*, *8*, 458. doi:10.3390/rs8060458.

Bracaglia, M., Ferrazzoli, P., & Guerriero, L. (1995). A fully polarimetric multiple scattering model for crops. *Remote Sensing of Environment*, *54*, 170–179. doi:10.1016/0034-4257(95)00151-4

Caltagirone, F., Capuzi, A., Coletta, A., De Luca, G.F., Scorzafava, E., Leonardi, R., … Esposito, P.G. (2014). The COSMO-skymed dual use earth observation program: Development, qualification, and results of the commissioning of the overall constellation. *IEEE Journal of Selected Topics in Applied Earth Observations and Remote Sensing*, *7*, 2754–2762. doi:10.1109/JSTARS.2014.2317287

Choker, M., Baghdadi, N., Zribi, M., El Hajj, M., Paloscia, S., Verhoest, N.E.C., … Mattia, F. (2017). Evaluation of the Oh, Dubois and IEM backscatter models using a large dataset of SAR data and experimental soil measurements. *Water*, *9*, 38. doi:10.3390/w9010038

Del Frate, F., Ferrazzoli, P., Guerriero, L., Strozzi, T., Wegmüller, U., Cookmartin, G., & Quegan, S. (2004). Wheat cycle monitoring using radar data and a neural network trained by a model. *IEEE Transactions on Geoscience and Remote Sensing*, *42*, 35–44. doi:10.1109/TGRS.2003.817200

Della Vecchia, A., Ferrazzoli, P., Guerriero, L., Blaes, X., Defourny, P., Dente, L., … Wegmuller, U. (2006). Influence of geometrical factors on crop backscattering at C band. *IEEE Transactions on Geoscience and Remote Sensing*, *44*, 778–790. doi:10.1109/TGRS.2005.860489

Dobson, M.C., Ulaby, F.T., Hallikainen, M.T., & El-Rayes, M.A. (1985). Microwave dielectric behavior of wet soil-part II: Dielectric mixing models. *IEEE Transactions on Geoscience and Remote Sensing*, *23*, 35–46. doi:10.1109/TGRS.1985.289498

Eom, H.J., & Fung, A.K. (1984). A scatter model for vegetation up to Ku-band. *Remote Sensing of Environment*, *15*, 185–200. doi:10.1016/0034-4257(84)90030-0

Ferrazzoli, P. (2002). *SAR for agriculture: Advances, problems and prospects.* Proceedings of the Third International Symposium on Retrieval of bio- and geophysical parameters from SAR data for land applications (pp. 47–56). Sheffield, UK: ESA SP 475.

Fung, A.K. (1994). *Microwave scattering and emission models and their applications.* Norwood, NJ, USA: Artech House.

Gherboudj, I., Magagi, R., Berg, A.A., & Toth, B. (2011). Soil moisture retrieval over agricultural fields from multi-polarized and multi-angular RADARSAT-2 SAR data. *Remote Sensing of Environment*, *115*, 33–43. doi:10.1016/j.rse.2010.07.011

Huang, Y., Walker, J.P., Gao, Y., Wu, X., & Monerris, A. (2016). Estimation of vegetation water content from the

radar vegetation index at L-band. *IEEE Transactions on Geoscience and Remote Sensing*, *54*, 981–989. doi:10.1109/TGRS.2015.2471803

Jia, M., Tong, L., Zhang, Y., & Chen, Y. (2013). Multitemporal radar backscattering measurement of wheat fields using multifrequency (L, S, C, and X) and full-polarization. *Radio Science*, *48*, 471–481. doi:10.1002/rds.v48.5

Karam, M.A., & Fung, A.K. (1988). Electromagnetic scattering from a layer of finite length,randomly oriented, dielectric, circular cylinders over a rough interface with application to vegetation. *International Journal of Remote Sensing*, *9*, 1109–1134. doi:10.1080/01431168808954918

Kim, S.B., Moghaddam, M., Tsang, L., Burgin, M., Xiaolan, X., & Njoku, E.G. (2014a). Models of L-band radar backscattering coefficients over global terrain for soil moisture retrieval. *IEEE Transactions on Geoscience and Remote Sensing*, *52*, 1381–1396. doi:10.1109/TGRS.2013.2250980

Kim, Y., Jackson, T.J., Bindlish, R., Hong, S., Jung, G., & Lee, K. (2014b). Retrieval of wheat growth parameters with radar vegetation indices. *IEEE Geoscience and Remote Sensing Letters*, *11*, 808–812. doi:10.1109/LGRS.2013.2279255

Lievens, H., & Verhoest, N.E.C. (2011). On the retrieval of soil moisture in wheat fields from L-band SAR based on water cloud modeling, the IEM, and effective roughness parameters. *IEEE Geoscience and Remote Sensing Letters*, *8*, 740–744. doi:10.1109/LGRS.2011.2106109

Mattia, F., Le Toan, T., Picard, G., Posa, F., D'Alessio, A., Notarnicola, C., & Pasquariello, G. (2003). Multitemporal C-band radar measurements on wheat fields. *IEEE Transactions on Geoscience and Remote Sensing*, *41*, 1551–1560. doi:10.1109/TGRS.2003.813531

Moran, M.S., Alonso, L., Moreno, J.F., Cendrero Mateo, M. P., de la Cruz, D.F., & Montoro, A. (2012). A RADARSAT-2 quad-polarized time series for monitoring crop and soil conditionsin Barrax, Spain. *IEEE Transactions on Geoscience and Remote Sensing*, *50*, 1057–1070. doi:10.1109/TGRS.2011.2166080

Oh, Y. (2004). Quantitative retrieval of soil moisture content and surface roughness from multipolarized radar observations of bare soil surfaces. *IEEE Transactions on Geoscience and Remote Sensing*, *42*, 596–601. doi:10.1109/TGRS.2003.821065

Paloscia, S., Santi, E., Fontanelli, G., Montomoli, F., Brogioni, M., Macelloni, G., … Pettinato, S. (2014). The sensitivity of cosmo-skymed backscatter to agricultural crop type and vegetation parameters. *IEEE Journal of Selected Topics in Applied Earth Observation and Remote Sensing*, *7*, 2856–2868. doi:10.1109/JSTARS.2014.2345475

Rava, D., Barber, M., Grings, F., & Karszenbaum, H. (2016). *Evaluación del desempeño de dos sistemas SAR aerotransportados sobre suelos agrícolas: SARAT (CONAE) y UAVSAR (NASA/JPL)*. Proceedings of 2016 IEEE Biennial Congress of Argentina (ARGENCON) (pp. 1–6). doi:10.1109/ARGENCON.2016.7585343

Skora, J.S., Sanz, A.J., & Fabbra, R.D.M. (2005). *Dual polarized phased array antenna for airborne L-band SAR*. Proceedings of SBMO/IEEE MTT-S International Conference on Microwave and Optoelectronics (pp. 192–196). doi:10.1109/IMOC.2005.1579975

Stamenkovic, J., Ferrazzoli, P., Guerriero, L., Tuia, D., & Thiran, J.-P. (2015). Joining a discrete radiative transfer model and a kernel retrieval algorithm for soil moisture estimation from SAR data. *IEEE Journal of Selected Topics in Applied Earth Observation and Remote Sensing*, *8*, 3463–3474. doi:10.1109/JSTARS.2015.2432854

Steele-Dunne, S.C., McNairn, H., Monsivais-Huertero, A., Judge, J., Liu, P.-W., & Papathanassiou, K. (2017). Radar remote sensing of agricultural canopies: A review. *IEEE Journal of Selected Topics in Applied Earth Observations and Remote Sensing*, *10*, 2249–2273. doi:10.1109/JSTARS.2016.2639043

Touré, A., Thomson, K.P.B., Edwards, G., Brown, R.J., & Brisco, B.G. (1994). Adaptation of the MIMICS backscattering model to the agricultural context-wheat and canola at *L* and *C* bands. *IEEE Transactions on Geoscience and Remote Sensing*, *32*, 47–61. doi:10.1109/36.285188